



# Quantifying cloud masking in a single column

Lukas Klufft<sup>1</sup>, Bjorn Stevens<sup>1</sup>, Manfred Brath<sup>2</sup>, and Stefan A. Buehler<sup>2</sup>

<sup>1</sup>Max Planck Institute for Meteorology, Hamburg, Germany

<sup>2</sup>Center for Earth System Research and Sustainability (CEN), Meteorological Institute, Universität Hamburg, Hamburg, Germany

**Correspondence:** Lukas Klufft (lukas.klufft@mpimet.mpg.de)

**Abstract.** We add idealized clouds into a single column model and show that the cloud radiative effects as observed from satellites can be reproduced by a combination of high and either low or mid-level clouds. To quantify all-sky climate sensitivity we define a “fixed-cloud-albedo” null hypothesis, which assumes an understanding of how cloud temperatures change, but assumes no change in cloud albedo. This null-hypothesis depends on how clouds are vertically distributed along the temperature profile and how this changes as the surface warms. Drawing only distributions which match the cloud radiative effects of present day observations yields a mean fixed-albedo (also keeping surface albedo fixed) climate sensitivity of 2.2 K, slightly smaller than its clear-sky value. This small number arises from two compensating effects: the dominance of cloud masking of the radiative response, primarily by mid-level clouds which are assumed not to change with temperature, and a reduction of the radiative forcing due to masking effect by high clouds. Giving more prominence to low-level clouds, which are assumed to change their temperature with warming, reduces estimates of the fixed-albedo climate sensitivity to 2.0 K. This provides a baseline to which changes in surface albedo, and a believed reduction in cloud albedo, would add to.

## 1 Introduction

The cloud-radiative effect is a significant contributor to Earth’s radiation balance (Hartmann and Short, 1980; Ramanathan et al., 1989). In the net it leads to a cooling of Earth’s surface as the contribution of clouds to the planetary albedo (Loeb et al., 2018), through scattering of visible radiation, is larger than their greenhouse effect, arising from their absorption of terrestrial radiation. This is expected given that the minimum temperature of the troposphere, and hence clouds, is much larger than zero, which more strongly bounds the strength of the cloud greenhouse effect as compared to the cloud albedo effect. This explains why changes in cloud albedo have more scope for influencing the climate, and why it is the focus of most studies that attempt to quantify the effect of clouds on climate sensitivity, i.e., the warming arising from a doubling of atmospheric concentrations of carbon dioxide.

However, even if the cloud coverage and albedo are held fixed with warming, the mere presence of clouds substantially influences Earth’s equilibrium climate sensitivity. It does so in two ways. First, high-clouds mask the radiative forcing in spectral regions (wave-numbers) where CO<sub>2</sub> emissions would otherwise arise from regions below the clouds. At these wave-numbers, and in these situations, the changing emission height arising from an increase in CO<sub>2</sub> will not be apparent at the top of the atmospheres – clouds get in the way. Second, clouds modify the radiative response to warming, by masking of emissions



in the spectral region known as the atmospheric window and by unmasking parts of the spectral response that they would have otherwise masked, or which would have been masked by water vapor (Stevens and Kluft, 2023).

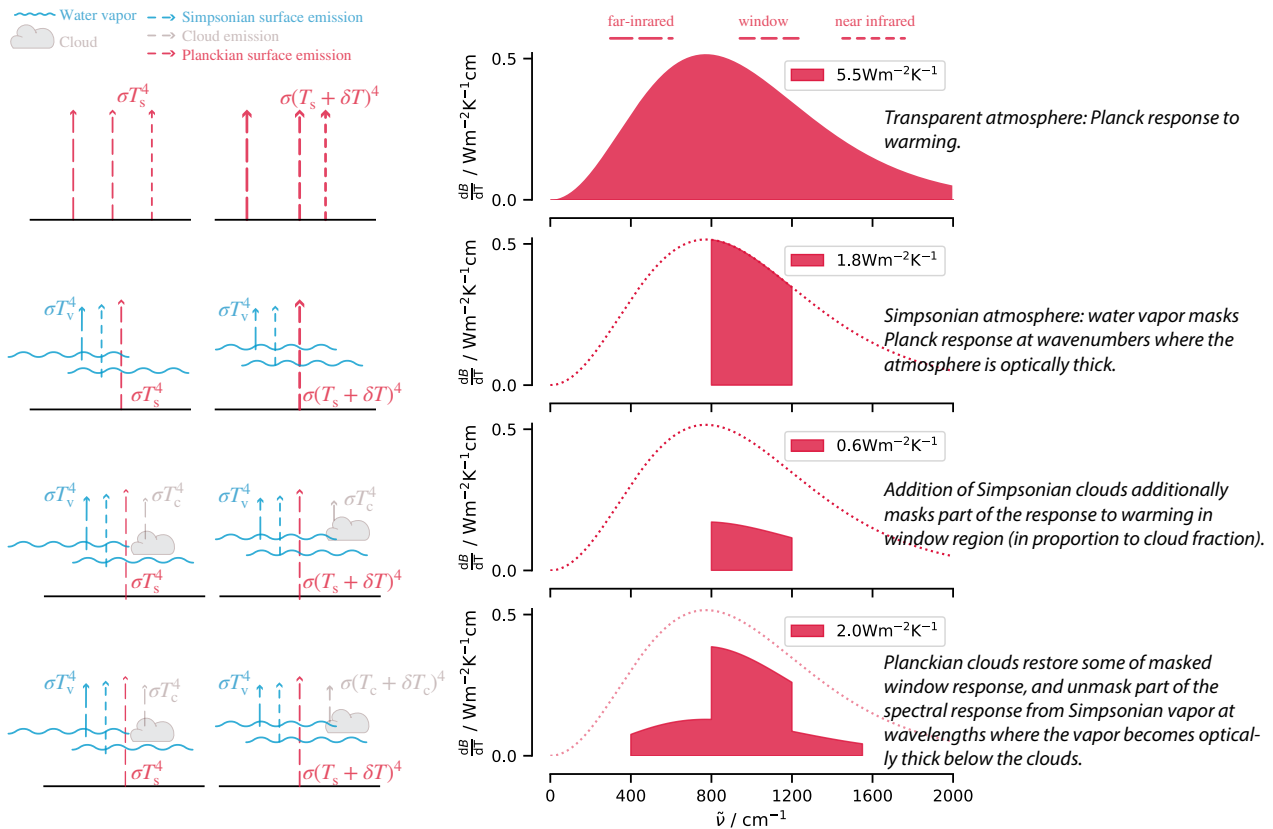


**Figure 1.** Conceptual framework showing how Simpsonian clouds and water vapor mask the radiative response at wavenumbers where they control the emission to space, and how part of the spectral response is restored from Planckian clouds.

The cloud masking of  $\text{CO}_2$  forcing is well appreciated and accounted for in the literature (Myhre et al., 1998); masking or unmasking of the clear-sky spectral response (Stevens and Kluft, 2023) is not. The basic ideas are illustrated conceptually with the help of the schematic in Fig. 1. Here we present the main ideas without accounting for the contributions of  $\text{CO}_2$  to the radiative response, although later, in our more detailed computations, these effects are included.

As is standard we define the atmospheric window as the range of wavenumbers ( $800 \text{ cm}^{-1}$ – $1200 \text{ cm}^{-1}$ ) where the atmosphere is optically thin through the entire column. Outside of this window, emission of radiant energy to space arises from water vapor (and  $\text{CO}_2$  were it to be considered). In these regions, the assumption of fixed relative humidity means that the optical thickness of the atmosphere, as measured downward from the top-of-the-atmosphere, depends on temperature, and hence emissions will not change with surface warming. We refer to this as a Simpsonian response (Ingram, 2010; Jeevanjee et al., 2010), which can be conceptualized as a spectral masking of the Planckian response that would otherwise arise from the



surface (Fig. 1, second row). Clouds, unlike water vapor, are gray across the thermal infrared. They thus control emissions at wavenumbers where the clear-sky emission would otherwise originate below them. Whether, and how much, they contribute to the radiative response to warming then depends on how or if they warm with the surface. Clouds which maintain a fixed temperature (Simpsonian clouds) further mask the spectral response that otherwise would have been expected in the window – reducing the radiative response to surface warming. Clouds that warm with the surface (Planckian clouds) substitute for the surface response within the window. If the change in cloud temperature is equal to the change in the surface temperature, then this mimics the surface response, albeit somewhat weakened by virtue of the clouds being at lower temperatures. Outside of the window, at wavenumbers where the emission height of water vapor lies below the clouds, the warming clouds can reclaim part of the spectral response which would have otherwise been masked by water vapor (Stevens and Kluft, 2023), as shown in the last row of Fig. 1.

We are interested in quantifying these effects for different scenarios of cloud changes, as doing so can provide a sense of how important the effects might be. Previous studies of course include these effects, but don't separate them from the clear-sky contributions to the radiative response to warming. For instance, a common approach to disentangle the cloud feedback is the partial radiative perturbation (PRP) method (Colman, 2003; Soden and Held, 2006). This method performs radiative transfer calculations with different atmospheric fields (e.g. temperature, humidity, clouds) independently varied, with the idea that this quantifies their impact on the radiation budget. Doing so differentiates the effects of changing different variables in coupled models, but ignores the cross-dependencies between variables. As a result the contribution to the radiative response from water vapor, as estimated by the PRP method, will depend on the assumed distribution of clouds; likewise adding and subtracting a given distribution of clouds will give different answers depending on the background distribution of water vapor.

In this study we explicitly account for masking and unmasking following Stevens and Kluft (2023). First, we start with a more precise description of how the atmosphere, and clouds, will change with warming, and then we calculate the changes in the irradiances with warming for an atmosphere with and without clouds. All of our estimates are performed using the single column model `konrad` (Kluft et al., 2019; Dacie et al., 2019). Because the radiative response varies linearly with the main state variables (Koll and Cronin, 2018; Bourdin et al., 2021; Kluft et al., 2021), the setting of a single column has proven to be quantitatively informative. We thus adopt it for our study. In `konrad` temperature changes with warming are specified to follow a moist adiabat, relative humidity is specified as constant, and clouds are, following Johnson et al. (1999), prescribed in three layers with properties chosen to match the observed radiation balance and our best understanding of how cloud-top temperatures will change with warming. Calculations with and without clouds allow us to quantify the cloud contribution to the climate sensitivity for the fixed-albedo null-hypothesis, whereby warming causes neither a change in cloud coverage, nor albedo (surface albedo is also held constant). By the reasoning reviewed above, the cloud effect will depend on how clouds are distributed, and how their temperatures (altitudes) change with warming, as well as the assumed distribution of water vapor. The aim of this study is to quantify this effect in a simple model as a basis for better understanding its potential importance for Earth's climate sensitivity.

Despite over forty years of satellite cloud observations, some basic properties of clouds remain uncertain. This makes it difficult to unambiguously construct a “global cloud scene”, that is also best representative of the cloud response to warming under



our ansatz of no change to their albedo. We approach the issue by creating a large ensemble of plausible cloud properties for the three layers of clouds to be considered, and sample the cloud configurations to select the subset consistent with global mean cloud-radiative effects observed with satellites (CERES, Loeb et al., 2018). Both the full ensemble of cloud properties and the plausible sub-sample are then used to quantify the cloud masking effect on the radiative forcing, and their masking/unmasking effect on the radiative response.

Accounting for clouds in this manner provides a more nuanced view on how clouds contribute to climate sensitivity, which should help guide observational programmes. It also extends a growing literature devoted to better understanding the climate sensitivity of a cloud free atmosphere, (e.g., Koll and Cronin, 2018; Seeley and Jeevanjee, 2021; Kluft et al., 2021), to include the effects of clouds under certain well defined limits, e.g., following Stevens and Kluft (2023). In Section 2 we elaborate on the implementation. In Section 3 we discuss the simulated cloud-radiative effect in present-day conditions as well as the cloud response to warming. Section 4 discusses in which aspects our perspective on cloud feedbacks differs and agrees with existing frameworks.

## 2 Modeling clouds in one dimension

We represent a trimodal cloud configuration using `konrad`, a python based one-dimensional radiative-convective equilibrium (RCE) model developed by Kluft et al. (2019). In our set-up surface temperatures are prescribed, and the tropospheric temperature profile is adjusted to follow a moist adiabat following the surface temperature. Above the convective-top the temperature profile is equilibrated into a radiative equilibrium which allows us to capture changes in cold-point temperatures. This approach greatly reduces the computational burden as it avoids the need to equilibrate the surface temperature (Romps, 2020).

All-sky fluxes are calculated using a two-stream correlated- $k$  representation of radiative transfer, RRTMG (Mlawer et al., 1997). Our previous work has shown RRTMG to compare well against line by line calculations within this same framework, and for the temperature ranges considered here (Kluft et al., 2021). RRTMG computes fluxes for completely overcast or clear-sky scenes. In overcast scenes, clouds are represented in terms of their pressure and temperature, optical depth, single scattering albedo and asymmetry parameter, with the optical properties represented as a function of an assumed cloud phase, condensate burden, and effective radius. All sky fluxes are constructed by weighted averages between clear and overcast scenes depending on the fractional weight of each.

Clouds are prescribed in three layers with distinct properties and behaviour in each layer. A low-level cloud-layer is introduced to represent boundary layer clouds, and its cloud-top temperature changes following a fixed anvil pressure (FAP), which due to the assumption of the moist adiabat means they will warm slightly more than the surface; a mid-level cloud layer is introduced at the melting level and is assumed to maintain a fixed anvil temperature (FAT); and a high-level cloud layer is tied to the level of the maximum of the radiatively driven convergence in clear skies (PHAT). This approach allows the cloud-altitude to be precisely defined for different background climates. Therefore, we can use two simulations with differing surface temperatures  $T_s = 285$  K and 291 K to compute the radiative feedback including the cloud-altitude feedback.



105 We assume that the overlap among clouds in different layers is random, which defines  $2^3$  different cloud configurations – each of which can lead to markedly different cloud radiative effects. In global circulation models (GCMs), this variability is parameterised by, e.g. the Monte-Carlo Independent Column Approximation (MCICA). This is effective when the radiation scheme is called often in time, as the sample noise is unbiased and averages out with high-temporal sampling. For our purposes, the limited number of cloud layers, and hence the smallness ( $2^3$ ) of the configuration space allows for a simpler approach. Let  
 110  $i \in \{1 \dots 8\}$  index each cloud combination, such that  $i = 1$  denotes clear skies,  $i = 2$  denotes only high clouds, and so on, as illustrated in Fig. 2. The probability of a given combination of clouds is then given as

$$P_i = \prod_{j=1}^3 P_{ij} \quad (1)$$

with  $P_{ij}$  being the probability that cloud-layer  $j$  is seen in cloud combination  $i$ , it can be expressed as follows:

$$P_{ij} = |1 - p_j - c_{ij}| \quad (2)$$

115 with binary cloud flag  $c_{ij}$ , which states if cloud layer  $j$  is present in combination  $i$ , and assumed cloud fraction  $p_j$ . The resulting weight  $P_i$  quantifies the probability of a given cloud combination based on the cloud fraction of the participating cloud layers. The all-sky radiative fluxes are then given by the weighted average of the individual cloud-overcast scenes (Figure 2).

$$F = \sum P_i F_i. \quad (3)$$

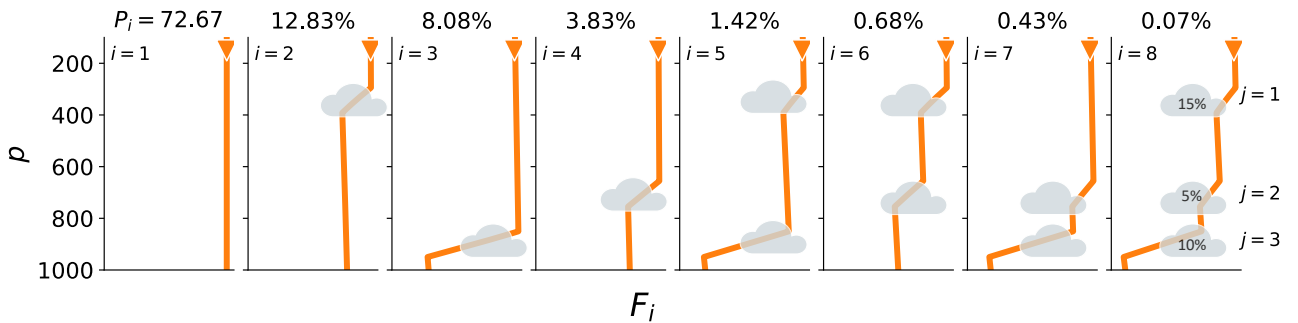


**Figure 2.** Schematic of all possible cloud-layer combinations  $i$  in a trimodal cloud distribution. In addition, the different impact on the downwelling shortwave flux is shown as orange line. The percentages on top state the probability  $P_i$  for each cloud-layer combination assuming random overlap and exemplary cloud fractions (shown in the right most panel).

To perform the calculations we need to make a choice for the cloud fraction, the integrated condensate path for each cloud  
 120 layer, and the effective radius. The particle phase, which influences how these physical properties are translated into optical properties is prescribed for each layer, with low- and mid-level clouds being treated as liquid and high clouds being treated as ice, and with no change in the phase of the different layers with warming. Because the clouds in the 1-D context represent an effective cloud, even if we could measure these properties from clouds globally, it is not clear that their mean would



125 be appropriate for the specification of an effective cloud. Therefore, we construct a large Monte-Carlo ensemble (MCE) by randomly drawing parameter values from values taken from a uniform prior distribution over the specified range.

130 Table 1 lists the range of possible values for each cloud property, from which we construct the MCE. We perform 32768 simulations, each of which comprises sixteen radiative transfer calculations (once for the warm and control temperature for each of the 8 configurations), with parameters chosen randomly from the parent distribution. The result is an ensemble of 32768 cloud scenes that describe the all-sky radiation budgets following the prior distribution of cloud parameters. Many of these scenes will, however, not result in plausible representations of Earth's top of the atmosphere radiation budget, as observed from satellite. Therefore, we construct an a posteriori distribution by sub-sampling the ensemble to find cloud configurations whose cloud-radiative effect (CRE) is consistent with satellite observations. This defines a plausible set of cloud scenes, which we then use to quantify various cloud-radiative metrics in both the present and a warmer climate.

Quantity	Unit	Value
Effective radius (liquid)	$\mu\text{m}$	10
Effective radius (ice)	"	50
High cloud fraction	%	1–35
Mid cloud fraction	"	"
Low cloud fraction	"	"
IWP high cloud	$\text{g m}^{-2}$	2–75
LWP mid-level cloud	"	20–200
LWP low cloud	"	2–200

**Table 1.** Possible value range for physical and optical cloud parameters in the MCE.

### 3 Cloud radiative effects

#### 135 3.1 The current climate

In a first step, we quantify how the presence of clouds impacts Earth's radiant energy budget for the control temperature, and use these effects to sample a plausible parameter range for the prescribed clouds. Cloud radiative effects are compared to the summary values for the July 2005–June 2015 period as provided by the Clouds and Radiant Energy Systems (CERES) EBAF Ed4.0 product (Loeb et al., 2018, Tab. 5).

140 Figure 3 presents the longwave, shortwave, and net CRE for the full ensemble (light colors). Unsurprisingly, values for the net CREs and its components spread across a very large range of values. For example, the  $\text{CRE}_{\text{net}}$  can reach values be-



tween  $-83 \text{ W m}^{-2}$ – $28 \text{ W m}^{-2}$ . That the ensemble mean is in good agreement with the CERES data suggests that the uniform distributions for the variable parameters were centered around sensible values.

As a next step, we sub-sample the full ensemble to select cloud configurations in which all three CRE values are within  
145  $\pm 5 \text{ W m}^{-2}$  of the CERES values at the top-of-the-atmosphere – which we refer to as “plausible” values. Tests with narrower acceptance showed no qualitative difference but greatly reduced the output statistics. Even with this relatively loose constraint on acceptable values of the SW, LW and net CRE, requiring all three to be satisfied reduces the ensemble to 786 out of 32786 cloud scenes (about 2.4 %). Parameter distributions for the subset of parameters leading to plausible CRE are described by the 5<sup>th</sup>, 50<sup>th</sup>, and 95<sup>th</sup> percentiles of their distributions and listed in Table 2. The a posteriori distributions show that the CRE from  
150 CERES most strongly constrains the property of high-level clouds.

Since the effective parameters found to capture the observed CRE are found to be similar to parameters characteristic to observed clouds, it is justified to use an effective cloud to model the globally averaged effect of broad cloud distributions. The average cloud fraction is 18 % for high clouds and 20 % for mid-level clouds and 17 % for low clouds, which are not unreasonable values. The coverage of mid-level clouds is higher than expected, but could be interpreted as representative of  
155 cloud populations in the mid-latitudes. The plausible range for the mid-level and low-level cloud parameters is not substantially reduced relative to their initial distributions, this might be indicative of the capability of the two cloud types to compensate for one another.

To test the possibility of compensation we further investigate the impact of individual cloud layers by performing three additional sets of simulations. In each of these we omit one of the three cloud layers. Results are presented in Figure 3. The  
160 strongest impact is seen in the simulation without high clouds. In absence of high clouds, which are characterized by their cold cloud-top, the longwave CRE almost vanishes. As a result, the net CRE is much more negative (about  $-40 \text{ W m}^{-2}$  on average), and can no longer be reconciled with the CERES data. The calculations also confirm the ability of increased low-level clouds to compensate for mid-level clouds and vice versa. Table 2 further demonstrates that for two cloud layers, the cloud parameters of the lower cloud layers become more constrained than for the case of three layers. In the absence of either the mid- or low-level  
165 clouds, Figure 3 indicates that strongly negative  $\text{CRE}_{\text{SW}}$  are no longer possible, which makes it more difficult to find samples that reproduce the observed  $\text{CRE}_{\text{SW}}$ , increasingly so in the absence of low clouds.

We conclude that a single column model with an idealized trimodal cloud distribution is able to produce CREs that are in good agreement with the best available observations of Earth’s radiant energy budget. Our calculations demonstrate that the presence of high clouds is essential for a realistic longwave CRE. Low- and mid-level clouds while important, act in a similar  
170 way, making it easier for them to compensate for one another. The CRE at the top-of-the-atmosphere is unable to distinguish between low-level and mid-level cloud amounts. This limitation has significant implications for understanding how the system responds to global warming, as modeled in our study. Specifically, our model shows that mid-level clouds mask the radiative response to warming, whereas low-level clouds, which warm in tandem with the surface (as prescribed in the model), are also effective at enhancing the spectral response to warming.

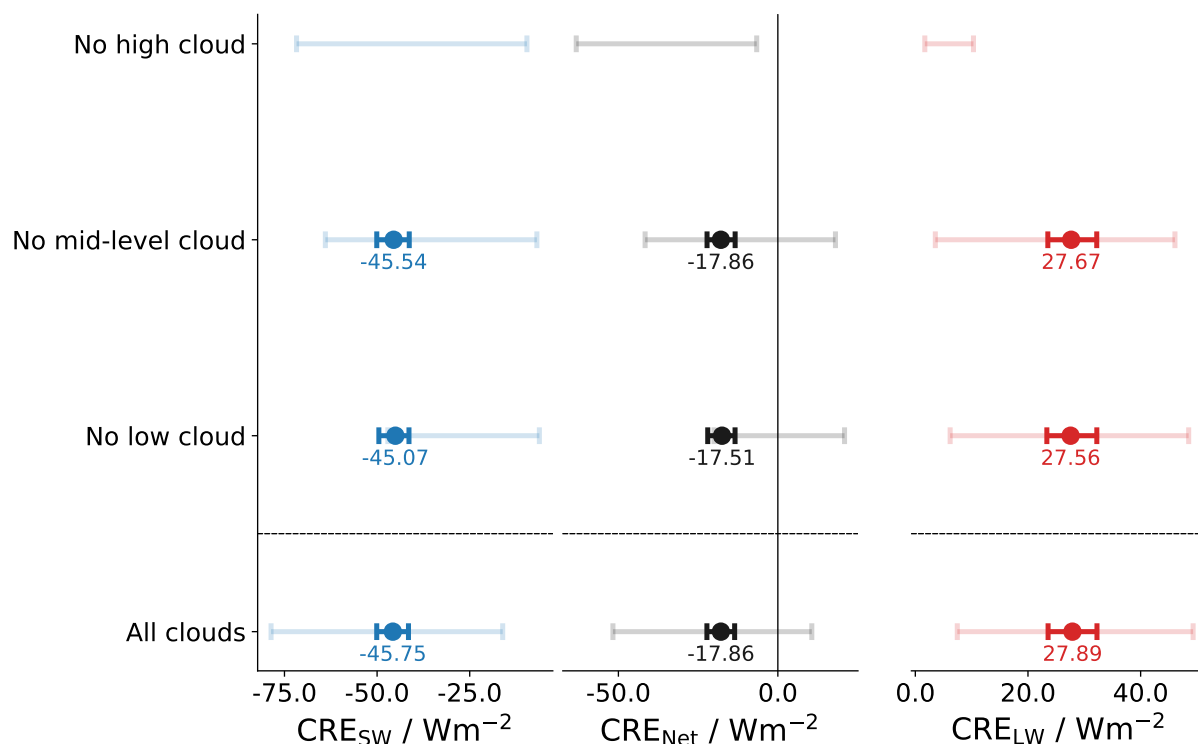


**Figure 3.** Distribution of the shortwave cloud-radiative effect  $CRE_{SW}$ , the net cloud-radiative effect  $CRE_{Net}$ , the longwave cloud-radiative effect  $CRE_{LW}$ . The faded lines depict the 5%–95% interval of all possible CRE values in the full ensemble. The bold lines show the same range, but for a plausible subsample that is in agreement with satellite observations.

### 175 3.2 Response to surface warming

In this section we quantify how our representation of clouds modifies the model’s clear-sky response to forcing, the radiative response to warming, and their quotient, the climate sensitivity.

In exploring how clouds with both a fixed coverage, and a fixed albedo (and hence phase), affect the estimate of climate sensitivity we are exploring a form of state dependence, with the cloud distribution being the important state parameter. Past studies, using methods like PRP, would have subsumed these effects into estimates of the clear-sky sensitivity. Our approach allows for a more full accounting of clouds, and by implication allows us to assess how errors in the distribution of clouds, or estimates of changes in cloud temperature, will effect estimates of climate sensitivity.

The calculations involve additional simulations, based on the MCE of cloud scenes. In a first step, we double the  $CO_2$  concentration while keeping a fixed  $T_s = 288K$ . After letting the stratosphere adjust to the new gaseous composition, we can directly quantify the adjusted radiative forcing as

$$\Delta F = F_{2 \times CO_2} - F_{CO_2} \quad (4)$$





with  $F_x$  being the outgoing longwave radiation for a  $\text{CO}_2$  mixing ratio  $x$ .

We find that clouds reduce the radiative forcing by about  $0.7 \text{ W m}^{-2}$ , or by about 15 % of the clear-sky value of  $4.5 \text{ W m}^{-2}$  (see bottom row of Figure 4). This masking is solely done by high clouds, because the cloud needs to be located above the emission height of  $\text{CO}_2$  to effectively mask the radiative forcing. In the absence of high clouds  $\Delta F$  is close to the clear-sky value (see top row of Figure 4). By constraining our MCE to plausible cloud combinations (bold lines), we find that the reduction in  $\Delta F$  is a robust signal and, on its own, would reduce the fixed-albedo climate sensitivity by about 0.5 K.

In a second step, we estimate how clouds influence the radiative response to forcing,  $\lambda$ . We quantify this by repeating our simulations at  $T_s = 285 \text{ K}$  and  $291 \text{ K}$ . Using the two sets of simulations at different  $T_s$ , we define the feedback parameter as

$$\lambda = \frac{F_{291\text{K}} - F_{285\text{K}}}{6\text{K}}, \quad (5)$$

with  $F_T$  denoting the net irradiance at the top-of-atmosphere for the given temperature  $T$ .

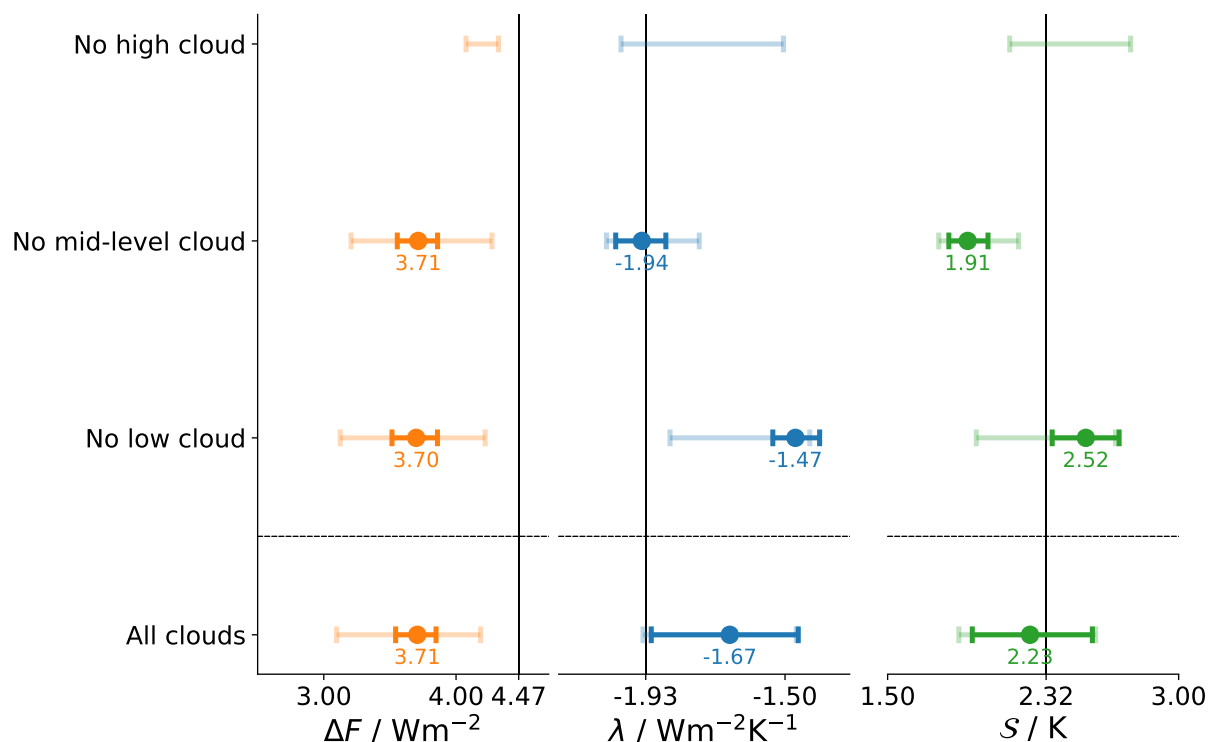
In each of the simulations the different cloud levels adjust their cloud-top altitude based on the thermodynamic profiles of the atmosphere (see Section 2). This means that low-level clouds remain at the same pressure level, mid-level clouds move upward following the melting level, and high-level clouds move upward following the level where the divergence of the radiatively driven subsidence maximizes. As a result both high and low-clouds warm with the surface, high-level clouds somewhat less so, while mid-level clouds remain at the same temperature. The different behavior of mid- and low-level clouds helps quantify to what extent an uncertain temperature response of clouds to surface warming affects the sensitivity of the system to forcing – effectively providing a first estimate of uncertainty introduced by clouds, even if their coverage remains unchanged.

Figure 4b presents  $\lambda$ . Clouds reduce the radiative response to warming, increasing  $\lambda$  from its clear-sky value of  $-1.9 \text{ W m}^{-2} \text{ K}^{-1}$  to  $-1.7 \text{ W m}^{-2} \text{ K}^{-1}$ . This alone would result in an increase of the equilibrium climate sensitivity  $\mathcal{S}$ . This effect, however, is less than that of changes in  $\Delta F$ , which reduces from  $4.5 \text{ W m}^{-2}$  to  $3.7 \text{ W m}^{-2}$ . Hence, for the fixed-albedo null hypothesis, clouds slightly reduce  $\mathcal{S}$  relative to its clear-sky value. Following the arguments of Stevens and Kluff (2023) this is expected to the extent that clouds unmask parts of the spectral response to warming that would otherwise be masked by water vapor. Comparing the no mid-level versus the no low-level cloud response shows that low-level clouds are responsible for this unmasking, as in their absence the radiative response to warming is much smaller, and  $\mathcal{S}$  increases by 0.2 K (Fig. 4 over its clear-sky value of 2.3 K). Conversely, in the absence of mid-level clouds, the increase in low-level clouds, which in our model warm slightly more than the surface, enhances the radiative response to warming reducing  $\mathcal{S}$  by 0.3 K relative to its clear-sky value.

In summary, the net effect on  $\lambda$  is sufficient to balance the reduction in  $\Delta F$  resulting in an equilibrium climate sensitivity  $\mathcal{S} = -\Delta F/\lambda$  in the range of 1.94 K–2.56 K. This range encompasses the clear-sky value of 2.3 K, but more often leads to less rather than more warming. This outcome arises because, in our ansatz, the cloud masking effect on  $\Delta F$  largely compensates that on  $\lambda$ , while the unmasking effect only influences  $\lambda$ , thereby reducing  $\mathcal{S}$ .

#### 4 Discussion

One aspect of clouds, which will be present even when their coverage and albedo does not change, is their ability to mask surface albedo changes. Pistone et al. (2014) estimate an all-sky radiative response to surface albedo changes that is 5/8ths of



**Figure 4.** Distribution of the adjusted radiative-forcing  $\Delta F$ , the climate feedback parameter  $\lambda$ , the equilibrium climate sensitivity  $S$ . The faded lines depict the 5%–95% interval of all possible CRE values in the full ensemble. The bold lines show the same range, but for a plausible subsample that is in agreement with satellite observations. Vertical lines mark the respective value at clear-sky conditions.

220 the clear-sky response. Thus an all-sky feedback estimate of  $0.35 \text{ W m}^{-2} \text{ K}^{-1}$  (Forster et al., 2021) implies a clear-sky feedback of  $0.56 \text{ W m}^{-2} \text{ K}^{-1}$ . This would raise the best estimate of the fixed atmosphere-albedo clear-sky sensitivity to  $3.26 \text{ K}$ , and the fixed atmosphere-albedo all-sky sensitivity to  $2.8 \text{ K}$ . This demonstrates that fixed-albedo clouds reduce the climate sensitivity even more when surface albedo changes are incorporated.

Our “null hypothesis” for high clouds is comparable to the T-FRAT framework by Yoshimori et al. (2020). They argue that 225 to quantify the effect of changes in cloud properties one needs to account for fundamental feedbacks in their thermodynamic surrounding. This happens naturally in our framework, which focuses on how clouds change their temperature. It also leads us to conclude, similarly to Yoshimori et al. (2020), that the presumption of a strong cloud-altitude feedback under PHAT largely compensates for the un-physical presumption that high-clouds won’t rise as the troposphere deepens with warming.

Our study does not account for changes in cloud fraction. This is a deliberate choice as, in contrast to the cloud altitude, 230 there is no conceptual framework that would allow us to predict the cloud fraction in our one-dimensional model. However, our findings open a new perspective on the impact of changing high-cloud fractions. Usually, for these high cirrus, a balancing longwave and shortwave effect is thought to result in a close to zero net feedback (Ceppi et al., 2017, and references therein).



Our results, moreover, suggest that an increase of high clouds would also increase the masking of the radiative forcing and hence a lower climate sensitivity.

## 235 5 Conclusions

We propose a “null hypothesis” for cloud-altitude changes in a warming climate, and use this to calculate the fixed-albedo climate sensitivity. Our hypothesis is rooted in the assumption that different cloud types respond to surface warming in different ways: low-level clouds are assumed to be tied to a fixed pressure, mid-level clouds to the freezing level, and high-level clouds to the level of maximum clear-sky subsidence divergence. We add this conceptual representation of clouds to the one-dimensional  
240 RCE model `konrad` to quantify how, if they were to behave in the manner posited, they would affect the radiative response to forcing.

Satellite observations show that the presence of cloud cools the current climate by adding a net CRE of about  $-17 \text{ W m}^{-2}$ . We use this to construct a MCE to demonstrate that a trimodal vertical cloud distribution can adequately simulate the observed CRE, with ambiguity in the distribution of low- versus mid-level clouds. The measurements provide a much stronger constraint  
245 to high clouds.

In addition, clouds, even if they do not change their albedo, alter the Earth’s climate sensitivity, i.e., its warming in response to a  $\text{CO}_2$  doubling. On one hand, they mask the radiative forcing by about  $0.7 \text{ W m}^{-2}$ , thus decreasing the climate sensitivity by about 15%. On the other hand, they both mask and unmask the radiative response to warming, with the latter slightly more dominant on average, so as to increase the expected response by  $0.2 \text{ W m}^{-2} \text{ K}^{-1}$ , an increase that is almost exactly canceled  
250 when the effect of clouds on the masking of surface albedo is considered. Our calculations thus suggest that in the absence of changes in cloud albedo, the difference between the all sky and clear-sky climate sensitivity is about zero.

*Code availability.* `konrad v1.0.2` is available on <https://doi.org/10.5281/zenodo.7438306>.

*Author contributions.* The presented concepts and ideas have been developed jointly by all authors. LK has performed the analysis, created the figures, and written the original draft. BS has created the schematic of the cloud masking. MB has developed the algorithm to compute  
255 the all-sky fluxes.

*Competing interests.* We are not aware of any competing interests.



## References

- Bourdin, S., Kluft, L., and Stevens, B.: Dependence of Climate Sensitivity on the Given Distribution of Relative Humidity, *Geophys Res Lett*, 48, <https://doi.org/10.1029/2021GL092462>, 2021.
- 260 Ceppi, P., Brient, F., Zelinka, M. D., and Hartmann, D. L.: Cloud feedback mechanisms and their representation in global climate models, *WIREs Clim Change*, 8, <https://doi.org/10.1002/wcc.465>, 2017.
- Colman, R.: A comparison of climate feedbacks in general circulation models, *Climate Dynamics*, 20, 865–873, <https://doi.org/10.1007/s00382-003-0310-z>, 2003.
- Dacie, S., Kluft, L., Schmidt, H., Stevens, B., Buehler, S. A., Nowack, P. J., Dietmüller, S., Abraham, N. L., and Birner, T.: A 1D RCE study  
265 of factors affecting the tropical tropopause layer and surface climate, *Journal of Climate*, 32, 6769–6782, 2019.
- Forster, P., Storelvmo, T., Armour, K., Collins, W., Dufresne, J.-L., Frame, D., Lunt, D., Mauritsen, T., Palmer, M., Watanabe, M., Wild, M., and Zhang, H.: The Earth's Energy Budget, Climate Feedbacks, and Climate Sensitivity, in: *Climate Change 2021: The Physical Science Basis. Contribution of Working Group I to the Sixth Assessment Report of the Intergovernmental Panel on Climate Change*, edited by Masson-Delmotte, V., Zhai, P., Pirani, A., Connors, S., Péan, C., Berger, S., Caud, N., Chen, Y., Goldfarb, L., Gomis, M., Huang, M.,  
270 Leitzell, K., Lonnoy, E., Matthews, J., Maycock, T., Waterfield, T., Yelekçi, O., Yu, R., and Zhou, B., p. 923–1054, Cambridge University Press, Cambridge, United Kingdom and New York, NY, USA, <https://doi.org/10.1017/9781009157896.009>, 2021.
- Hartmann, D. L. and Short, D. A.: On the Use of Earth Radiation Budget Statistics for Studies of Clouds and Climate, *Journal of the Atmospheric Sciences*, 37, 1233–1250, 1980.
- Ingram, W.: A Very Simple Model for the Water Vapour Feedback on Climate Change: A Simple Model for Water Vapour Feedback on  
275 Climate Change, *Quarterly Journal of the Royal Meteorological Society*, 136, 30–40, <https://doi.org/10.1002/qj.546>, 2010.
- Jeevanjee, N., Seeley, J. T., Paynter, D., and Fueglistaler, S.: An Analytical Model for Spatially Varying Clear-Sky CO<sub>2</sub> Forcing, *Journal of Climate*, 34, 9463–9480, <https://doi.org/10.1175/JCLI-D-19-0756.1>, 2010.
- Johnson, R. H., Rickenbach, T. M., Rutledge, S. A., Ciesielski, P. E., and Schubert, W. H.: Trimodal Characteristics of Tropical Convection, *J. Climate*, 12, 2397–2418, [https://doi.org/10.1175/1520-0442\(1999\)012<2397:TCOTC>2.0.CO;2](https://doi.org/10.1175/1520-0442(1999)012<2397:TCOTC>2.0.CO;2), 1999.
- 280 Kluft, L., Dacie, S., Buehler, S. A., Schmidt, H., and Stevens, B.: Re-Examining the First Climate Models: Climate Sensitivity of a Modern Radiative–Convective Equilibrium Model, *Journal of Climate*, 32, 8111–8125, <https://doi.org/10.1175/JCLI-D-18-0774.1>, 2019.
- Kluft, L., Dacie, S., Brath, M., Buehler, S. A., and Stevens, B.: Temperature-Dependence of the Clear-Sky Feedback in Radiative-Convective Equilibrium, *Geophysical Research Letters*, 48, <https://doi.org/10.1029/2021GL094649>, 2021.
- Koll, D. D. B. and Cronin, T. W.: Earth's outgoing longwave radiation linear due to H<sub>2</sub>O greenhouse effect, *Proc. Natl. Acad. Sci. U.S.A.*,  
285 115, 10293–10298, <https://doi.org/10.1073/pnas.1809868115>, 2018.
- Loeb, N. G., Doelling, D. R., Wang, H., Su, W., Nguyen, C., Corbett, J. G., Liang, L., Mitrescu, C., Rose, F. G., and Kato, S.: Clouds and the Earth's Radiant Energy System (CERES) Energy Balanced and Filled (EBAF) Top-of-Atmosphere (TOA) Edition-4.0 Data Product, *Journal of Climate*, 31, 895–918, <https://doi.org/10.1175/JCLI-D-17-0208.1>, publisher: American Meteorological Society Section: Journal of Climate, 2018.
- 290 Mlawer, E. J., Taubman, S. J., Brown, P. D., Iacono, M. J., and Clough, S. A.: Radiative transfer for inhomogeneous atmospheres: RRTM, a validated correlated-k model for the longwave, *J. Geophys. Res.*, 102, 16663–16682, <https://doi.org/10.1029/97JD00237>, 1997.
- Myhre, G., Highwood, E. J., Shine, K. P., and Stordal, F.: New Estimates of Radiative Forcing Due to Well Mixed Greenhouse Gases, *Geophysical Research Letters*, 25, 2715–2718, <https://doi.org/10.1029/98GL01908>, 1998.



- Pistone, K., Eisenman, I., and Ramanathan, V.: Observational Determination of Albedo Decrease Caused by Vanishing Arctic Sea Ice, *Proceedings of the National Academy of Sciences*, 111, 3322–3326, <https://doi.org/10.1073/pnas.1318201111>, 2014.
- Ramanathan, V., Cess, R. D., Harrison, E. F., Minnis, P., and Barkstrom, B. R.: Cloud-Radiative Forcing and Climate: Results from the Earth Radiation Budget Experiment, *Science*, 243, 57–63, 1989.
- Romps, D. M.: Climate Sensitivity and the Direct Effect of Carbon Dioxide in a Limited-Area Cloud-Resolving Model, *Journal of Climate*, 33, 3413–3429, <https://doi.org/10.1175/JCLI-D-19-0682.1>, 2020.
- 300 Seeley, J. T. and Jeevanjee, N.: H<sub>2</sub>O Windows and CO<sub>2</sub> Radiator Fins: A Clear-Sky Explanation for the Peak in Equilibrium Climate Sensitivity, *Geophys Res Lett*, 48, <https://doi.org/10.1029/2020GL089609>, 2021.
- Soden, B. J. and Held, I. M.: An Assessment of Climate Feedbacks in Coupled Ocean–Atmosphere Models, *Journal of Climate*, 19, 3354–3360, <https://doi.org/10.1175/JCLI3799.1>, 2006.
- Stevens, B. and Kluft, L.: A Colorful Look at Climate Sensitivity, *Atmospheric Chemistry and Physics*, 23, 14 673–14 689, <https://doi.org/10.5194/acp-23-14673-2023>, 2023.
- 305 Yoshimori, M., Lambert, F. H., Webb, M. J., and Andrews, T.: Fixed Anvil Temperature Feedback: Positive, Zero, or Negative?, *Journal of Climate*, 33, 2719–2739, <https://doi.org/10.1175/JCLI-D-19-0108.1>, 2020.



Quantity	3 layers, percentiles			no mid, percentiles			no low, percentiles		
	5th	50th	95th	5th	50th	95th	5th	50th	95th
<b>Cloud fraction</b>									
high-level	0.13	0.18	0.27	0.16	0.21	0.30	0.12	0.16	0.23
mid-level	0.02	0.20	0.33	–	–	–	0.02	0.18	0.33
low-level	0.03	0.17	0.31	0.18	0.24	0.33	–	–	–
<b>Condensate burden (<math>\text{g m}^{-2}</math>)</b>									
high-level	12.39	38.42	66.72	12.77	38.38	66.74	12.41	40.76	67.53
mid-level	31.74	113.3	192.4	–	–	–	125.5	164.7	197.1
low-level	18.1	97.1	187.6	54.4	117.7	189.3	–	–	–

**Table 2.** Plausible value range for cloud amounts in the MCE.